

Rainfall Estimation Using Polarimetric Techniques at C-Band Frequencies

GIANFRANCO SCARCHILLI AND EUGENIO GORGUCCI

Istituto di Fisica dell'Atmosfera (CNR), Rome, Italy

V. CHANDRASEKAR

Colorado State University, Fort Collins, Colorado

THOMAS A. SELIGA

Electromagnetics and Remote Sensing Laboratory, Department of Electrical Engineering, University of Washington, Seattle, Washington

(Manuscript received 21 January 1992, in final form 2 December 1992)

ABSTRACT

The accuracy of radar measurements and their derived parameters, such as rainfall rate, are compromised by errors caused by propagation effects at C-band frequencies. The radar measurements of reflectivity factor Z and differential reflectivity Z_{DR} are affected by the absolute and differential attenuation through the rain medium. Another useful radar-derived parameter, differential propagation phase shift Φ_{DP} , is contaminated by the differential phase on backscatter δ , which attains significant values in rainfall at C-band frequencies. In this paper we present a technique to correct these propagation and backscatter effects by application of an algorithm that corrects first Z and Z_{DR} , using relationships between the specific and differential attenuations versus phase shift, which is followed by estimation of the differential backscatter phase shift parameter δ from the corrected Z_{DR} . Simulation results are presented to demonstrate the effectiveness of this correction procedure for two cases: (a) uniform rainfall along the path, and (b) rainfall varying with range. We also present estimates of accuracy in the measurement of radar-derived rainfall rates made after applying this correction procedure.

1. Introduction

The problem of rainfall estimation using S-band dual polarization radar technique has been studied by many researchers, for example, Seliga and Bringi (1976), Seliga and Bringi (1978), Bringi et al. (1982), Sachidananda and Zrnić (1986), Aydin et al. (1987). S-band radars have been most commonly used for rainfall estimation, since signals at S band generally suffer negligible attenuation due to propagation in rain. However, C-band radars have been popular for Doppler application due to their lower cost, greater mobility, and ease of installation and maintenance. More recently, many high-performance polarimetric radars have been built at C band due to their lower cost compared to their S-band counterparts, Schroth et al. (1988) and Leonardi et al. (1984). Though C-band radar systems are less expensive, radar signals at C band suffer significant attenuation as well as differential attenuation when used in the dual polarization mode. In addition to attenuation effects, the backscatter at horizontal H

and vertical V polarizations exhibits a phase difference between them, which can potentially affect differential propagation phase measurements. Hildebrand (1978) analyzed an iterative technique based on absolute reflectivity to estimate the attenuation in rain suffered by the radar-received signal. Aydin et al. (1989) developed an iterative procedure for estimating the attenuation at C-band frequencies based on reflectivity factor Z and differential reflectivity Z_{DR} measurements. Bringi et al. (1990) have examined the relationship between attenuation and differential phase measurements at microwave frequencies. This paper examines rainfall estimation procedures using a C-band dual-polarization radar, paying special attention to a procedure for correcting the rainfall estimates by accounting for the effects of absolute and differential attenuation as well as backscatter differential phase shift.

Our paper is organized so that section 2 outlines development of expressions for rainfall estimate using dual polarization reflectivity factor and phase measurements at C-band frequencies and examines the effects of propagation and differential backscatter phase on the rainfall estimates; section 3 describes a correction procedure for retrieving true reflectivity Z , differential reflectivity Z_{DR} , and differential propagation phase Φ_{DP} estimates from the radar measurements;

Corresponding author address: Dr. Gianfranco Scarchilli, Istituto di Fisica dell'Atmosfera (CNR), P. le Luigi Sturzo, 31, 00144 Rome, Italy.

section 4 contains an analysis of the limitations of the correction procedures due to the model and measurement fluctuations; and section 5 summarizes the paper's key results.

2. Dual polarization rainfall estimates at C band

The two most readily identifiable methods of rainfall estimation, using dual polarization radar measurements, are (a) use of reflectivity measurements at horizontal H and vertical V polarizations, and (b) use of differential propagation phase measurements Φ_{DP} . The distribution of raindrop sizes and shapes are of central importance in determining the electromagnetic scattering properties of rain-filled media. These effects, in turn, are embodied in the radar parameters of interest such as reflectivity factors $Z_{H,V}$; differential reflectivity Z_{DR} , which is the ratio of reflectivities at H and V polarization states (Seliga and Bringi 1976); and specific differential phase K_{DP} , which is due to the propagation phase difference between H and V polarization states (Seliga and Bringi 1978). Both cloud models and measurements of raindrop size distributions (RSD) at the surface and aloft show that a gamma distribution model adequately describes many of the natural variations in the RSD (Ulbrich 1983):

$$N(D) = N_0 D^\mu e^{-\Lambda D} \quad (\text{m}^{-3} \text{mm}^{-1}), \quad (1)$$

where $N(D)$ is the number of raindrops per unit volume per unit size interval (D to $D + \Delta D$), and (N_0 , Λ , μ) are parameters of the gamma distribution. A physically meaningful parameter known as the median volume diameter D_0 can be defined as

$$\int_0^{D_0} D^3 N(D) dD = \int_{D_0}^\infty D^3 N(D) dD. \quad (2)$$

Under this definition it can be shown that parameter Λ in (1) relates to (μ , D_0) by

$$\Lambda = \frac{3.67 + \mu}{D_0}. \quad (3)$$

The equilibrium shape of a raindrop falling at its terminal fall speed is determined by the balance between the forces due to surface tension, hydrostatic pressure, and aerodynamic pressure from airflow around the drop. The shapes of raindrops have been studied theoretically by Green (1975) and Beard and Chuang (1987), experimentally in wind tunnels by Pruppacher and Pitter (1971), and in natural rainfall using aircraft probes by Chandrasekar et al. (1988). All of the above studies show that the shape of a raindrop can be approximated by an oblate spheroid with the axis ratio (b/a) of the drop approximated by the relationship

$$\frac{b}{a} = 1.03 - 0.062 D_e, \quad (4)$$

where D_e is the equivolumetric spherical diameter of

a raindrop in millimeters, and a and b are the major and minor axes of the drop, respectively. Rainfall rate R and the radar parameters of the rain medium, namely, ($Z_{H,V}$, Z_{DR} , K_{DP}) can be expressed in terms of the RSD as follows:

$$R = 0.6\pi \times 10^{-3} \int D^3 N(D) v(D) dD \quad (\text{mm h}^{-1}), \quad (5)$$

where $v(D)$ is the fall speed of raindrop, which can be approximated as $v(D) = C_v D^{0.67}$ (Atlas and Ulbrich 1977):

$$Z_{H,V} = \frac{\lambda^4}{\pi^5 |k|^2} \int \sigma_{H,V}(D) N(D) dD \quad (\text{mm}^6 \text{m}^{-3}), \quad (6)$$

where $Z_{H,V}$ and $\sigma_{H,V}$ represent the reflectivity factors and radar cross sections at horizontal and vertical polarizations, respectively; λ the wavelength; and $K = (\epsilon_r - 1)/(\epsilon_r + 2)$ where ϵ_r is the refractive index of water:

$$Z_{DR} = \frac{\int \sigma_H(D) N(D) dD}{\int \sigma_V(D) N(D) dD}, \quad (7)$$

$$K_{DP} = \frac{180\lambda}{\pi} \text{Re} \int [f_H(D) - f_V(D)] N(D) dD, \quad (\text{deg km}^{-1}), \quad (8)$$

where f_H and f_V are the forward-scatter amplitudes at H and V polarization, respectively.

The radar measurements used in the dual polarization estimates of rainfall rates are Z_H ($\text{mm}^6 \text{m}^{-3}$) and Z_{DR} (dB) for the reflectivity-based technique (R_{DR}), and K_{DP} (deg km^{-1}) for the differential phase-based technique (R_{DP}). We can write expressions for R_{DR} and R_{DP} at C band as

$$R_{DR} = C_{DR} Z_H^\alpha Z_{DR}^\beta, \quad (9)$$

and

$$R_{DP} = C_{DP} K_{DP}^\nu. \quad (10)$$

The coefficients and the exponents in (9) and (10) need to be determined such that R_{DR} and R_{DP} estimate R with minimum error over a wide range of natural rainfall intensities. We vary the parameters of the RSD over a wide range as suggested by Ulbrich (1983) to obtain estimates of the coefficients C_{DR} , α , β , C_{DP} , and ν in (9) and (10). The parameter N_0 is varied between $10^{3.2-\mu} \exp(2.8\mu)$ and $10^{4.5-\mu} \exp(3.57\mu) \text{ m}^{-3} \text{mm}^{-1-\mu}$, D_0 is varied between 0.5 and 2.5 mm, and μ is varied between -1 and 4, nonintegers included. After computing ($Z_{H,V}$, Z_{DR} , K_{DP}) and R for each RSD and discarding the values of Z_H and R greater than 55 dBZ and 250 mm h^{-1} , respectively, a nonlinear regression

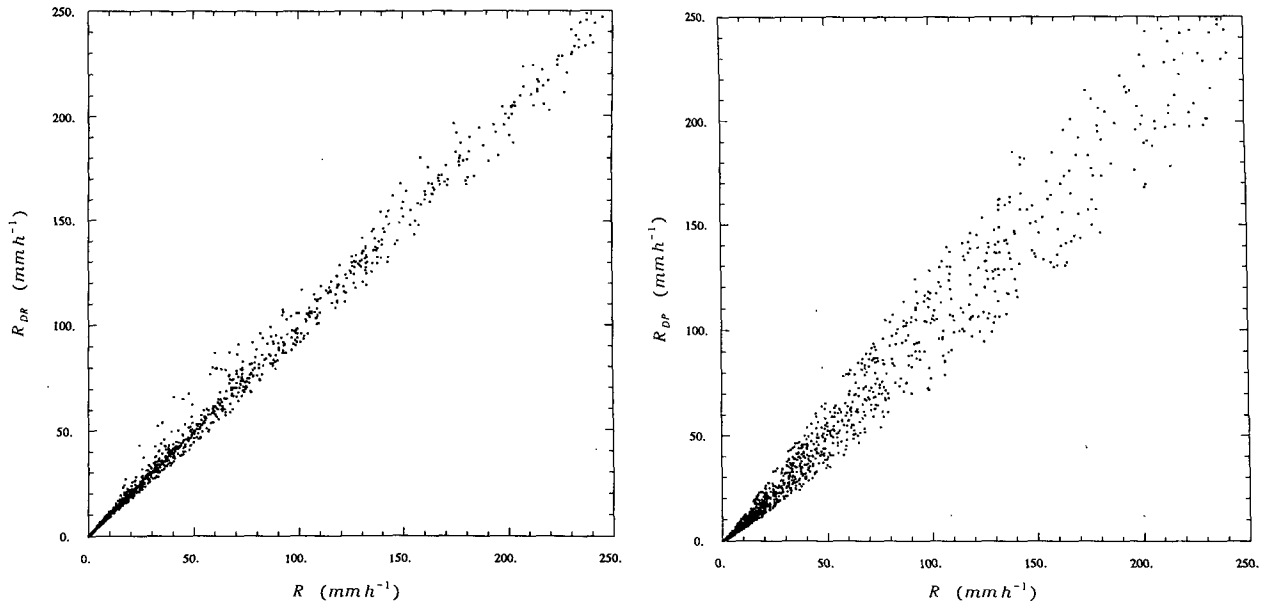


FIG. 1. (a) Scatterplot of the rainfall-rate estimate R_{DR} obtained from Z_H and Z_{DR} versus the actual rainfall rate R . (b) Scatterplot of the rainfall-rate estimate R_{DP} obtained from K_{DP} versus the actual rainfall rate R .

analysis is performed to estimate C_{DR} , α , β , C_{DP} , and ν . The best-fit relationship for R_{DR} is

$$R_{DR} = 3.61 \times 10^{-3} Z_H^{0.95} Z_{DR}^{-1.28}. \quad (11)$$

The coefficient ν obtained from the nonlinear regression procedure for R_{DP} was found to be nearly unity for C-band frequencies, and as a result we use R_{DP} of the form

$$R_{DP} = 19.8 K_{DP}. \quad (12)$$

Figure 1a shows the scatterplot of R_{DR} versus R , whereas Fig. 1b shows the scatter diagram of R_{DP} versus R . The average standard error of the data shown in Fig. 1a is 3.7 mm h^{-1} with a correlation coefficient of 0.998. The average standard error of the data shown in Fig. 1b is 8.2 mm h^{-1} with a correlation coefficient of 0.99. These values of average standard errors help in comparing the two techniques R_{DR} and R_{DP} . It has been shown qualitatively by Chandrasekar et al. (1990) that the average standard errors in the estimates of R_{DR} and R_{DP} vary with R for S-band measurements. We shall demonstrate similar results quantitatively for C-band radar estimates R_{DR} and R_{DP} .

Figure 2 shows the estimate of fractional standard error in R_{DR} and R_{DP} as a function of rain rate where the fractional standard error ϵ is defined as the standard error normalized with respect to its mean. We can see from Fig. 2 that the ϵ of R_{DR} is nearly constant up to $R = 50 \text{ mm h}^{-1}$; for $R > 50 \text{ mm h}^{-1}$ it decreases significantly. Figure 2 shows that the ϵ of R_{DP} is greater than ϵ of R_{DR} and decreases continuously with increasing rainfall rate over the entire range of R . It should be noted that the above results did not include possible

measurement errors in (Z_H , Z_{DR} , K_{DP}). The results change significantly in the presence of the measurement errors, as is shown in the scatter diagrams of Figs. 3a and 3b, corresponding to R_{DR} and R_{DP} versus R , respectively, with a number of sample pairs $N = 64$ and Doppler velocity spectrum width $w = 2 \text{ m s}^{-1}$. The results in Figs. 3a and 3b are obtained using the sim-

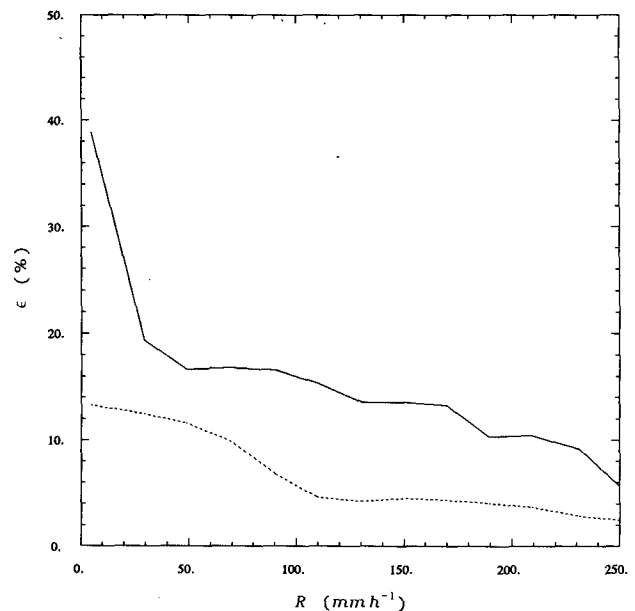


FIG. 2. Normalized standard error ϵ (%) as a function of the actual rain rate R . The dotted line refers to the standard error of the estimate R_{DR} and the solid line to standard error of the estimate R_{DP} .

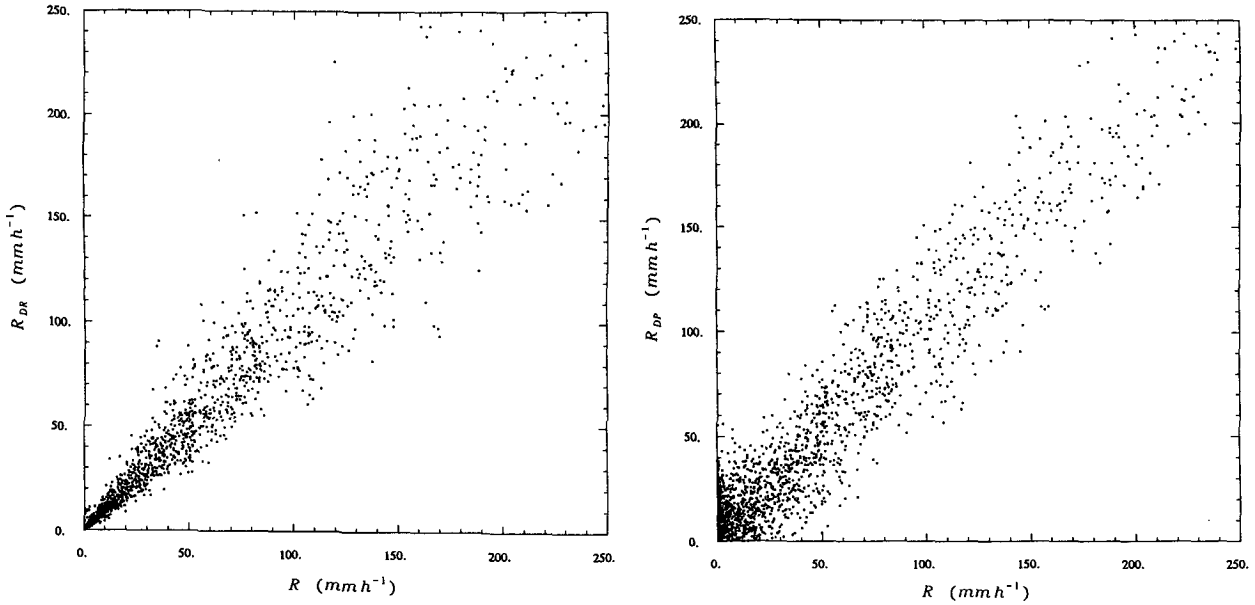


FIG. 3. (a) Scatterplot of estimate R_{DR} of rain rate with superimposed measurement error versus the actual rainfall rate R . (b) Scatterplot of estimate R_{DP} of rain rate with superimposed measurement error versus the actual rainfall rate R .

ulation procedure described by Chandrasekar et al. (1986). The average standard errors of the estimates R_{DR} and R_{DP} are comparable and equal to $14 mm h^{-1}$.

3. Effect of attenuation and backscatter phase on C-band measurements

Reflectivity measurements at C-band wavelengths are affected by attenuation of radar signals passing

through precipitation that exists between the radar and the measurement cell. Differential reflectivity measurements at C band are similarly affected by the differential attenuation between H and V polarized waves due to propagation through the same precipitation path. Figures 4a and 4b show scatterplots of specific attenuation α_H at horizontal polarization and differential attenuation α_D as a function of rainfall rate for the different RSD considered in the previous section.

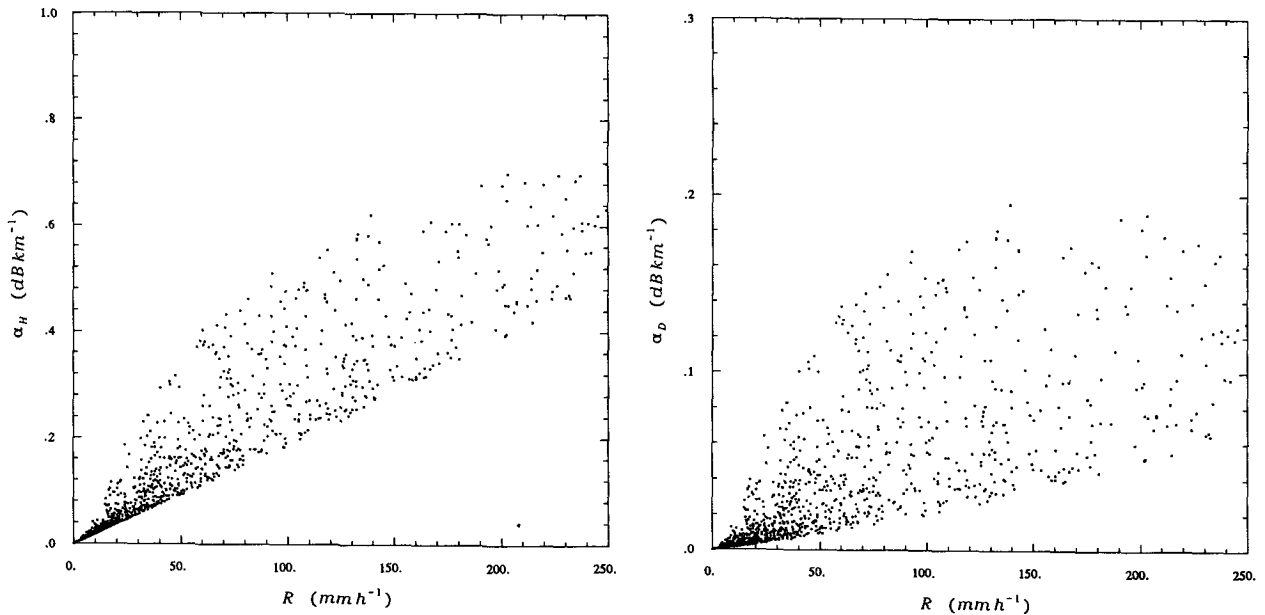


FIG. 4. (a) Scatterplot of specific attenuation α_H ($dB km^{-1}$) at horizontal polarization versus the actual rainfall rate R . (b) Scatterplot of differential attenuation α_D ($dB km^{-1}$) between horizontal and vertical polarization versus the actual rainfall rate R .

These results show that the absolute attenuation through extended rain cells could be easily several decibels in magnitude while comparable values of differential attenuation could reach as much as a few decibels.

The rain medium causes a differential propagation phase shift between H and V polarizations due to the nonspherical raindrops. This effect is observable, since the phase difference between the signals received at the H and V polarizations with a time lag between them can be corrected for the Doppler phase shift, thereby yielding an estimate of the differential propagation phase between the two polarizations H and V due to the medium between the radar and the measurement cell. This model (which works fairly well at S band) is not completely valid at C band, since there may be a significant phase difference δ between the polarizations due to the backscatter process. It can be shown that δ can typically range between values of 0° and 15° at C band. Thus the measured Φ_{DP} at C band is a combination of range cumulative Φ_{DP} , dependent on the propagation path, and δ which is a function of the measurement cell.

Absolute attenuation A_H and differential attenuation A_D perturb the measurements of Z_H and Z_{DR} , while backscatter differential phase shift δ perturbs the measurement of Φ_{DP} . Further, A_H , A_D , and Φ_{DP} are related to forward-scatter properties of the rain medium whereas Z_H , Z_{DR} , and δ are related to the backscatter properties. The real and imaginary part of the forward-scatter coefficients control the propagation phase and attenuation, respectively. This feature, combined with the fact that the raindrops become more nonspherical with increased size, makes the specific differential phase increase with increased specific attenuation and vice versa. Bringi et al. (1990) reported that on the average, both α_H and α_D can be estimated from K_{DP} through approximately linear relationships:

$$\alpha_H = 0.055K_{DP}, \quad \text{and} \quad (13)$$

$$\alpha_D = 0.013K_{DP}. \quad (14)$$

The range-cumulative two-way differential phase shift, attenuation, and differential attenuation can be expressed as

$$\Phi_{DP} = 2 \int_0^{R_c} K_{DP}(r) dr, \quad (15)$$

$$A_H = 2 \int_0^{R_c} \alpha_H(r) dr, \quad (16)$$

$$A_D = 2 \int_0^{R_c} \alpha_D(r) dr, \quad (17)$$

where R_c is the radar range to the observation cell. Since α_H and α_D are nearly linearly related to K_{DP} in rainfall, we can estimate A_H and A_D directly from Φ_{DP} measurements assuming no effect due to δ .

Similar to the relationship between α_H , α_D , and K_{DP} , the differential backscatter properties Z_{DR} and δ are also related as shown in the scatterplot of δ versus Z_{DR} in Fig. 5. These two parameters are very nicely inter-related, suggesting that we can estimate δ from Z_{DR} measurements, again provided that neither are affected by propagation effects. The relationship in Fig. 5 can be approximated by the polynomial expression

$$\delta = 0.41 - 0.97Z_{DR} + 0.37Z_{DR}^2 + 0.11Z_{DR}^3. \quad (18)$$

Thus, we have a fully coupled set of variables (Φ_{DP} , Z_H , Z_{DR}) where each is perturbed by either backscatter or propagation effects. In the next section we suggest a simple procedure to correct (Φ_{DP} , Z_H , Z_{DR}) to obtain their intrinsic values unaffected by backscatter and propagation effects.

4. Correction procedure for Z_H , Z_{DR} , and Φ_{DP}

We have seen in the previous section that (Z_H , Z_{DR}) measurements perturbed by attenuation and differential attenuation can be potentially corrected using intrinsic differential phase measurements which are unaffected by δ . Measurements of Φ_{DP} are perturbed by δ , however, which leads to a set of coupled parameters. We suggest a simple correction procedure that can be eventually extended as an iterative approach. The correction procedure can be simplified further if we use a second-degree polynomial to express δ as a function of Z_{DR} . The simplified correction procedure based on this approximation is given in the Appendix. The perturbation of Φ_{DP} by δ is an effect that is specific to a given range and can therefore change with range

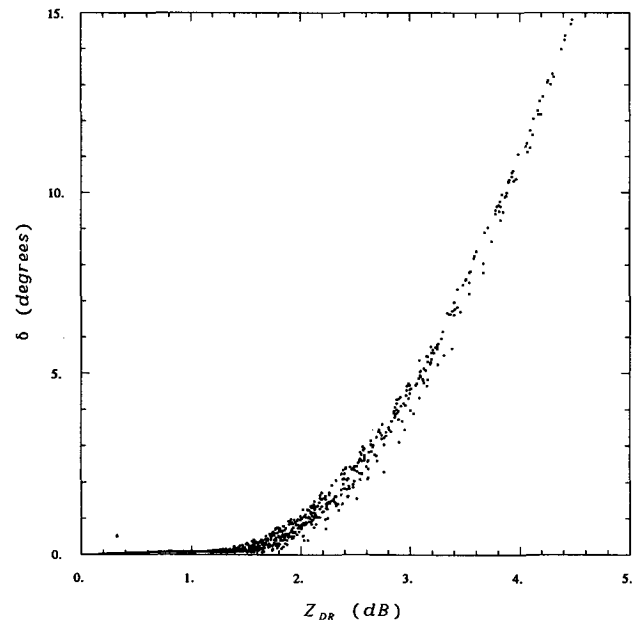


FIG. 5. Scatterplot of the differential reflectivity Z_{DR} (dB) versus the backscatter differential phase δ (deg).

independently. However, the perturbations of Z_H by A_H and Z_{DR} by A_D are range-cumulative effects and can change their values at any range, even though α_H and α_D may be negligible at any specific range of observations. We define the variables associated with the correction procedure as follows:

- Φ_{DP}^M, K_{DP}^M measured differential phase and specific differential phase,
- Φ_{DP}, K_{DP} intrinsic differential phase and specific differential phase,
- $\hat{\Phi}_{DP}, \hat{K}_{DP}$ estimate of intrinsic differential phase and specific differential phase,
- Z_H^M, Z_{DR}^M measured reflectivity factor at horizontal polarization and differential reflectivity,
- Z_H, Z_{DR} intrinsic reflectivity factor at horizontal polarization and the differential reflectivity,
- \hat{Z}_H, \hat{Z}_{DR} estimates of intrinsic Z_H and Z_{DR} after the correction,
- $\hat{\delta}$ estimate of differential backscatter phase based on \hat{Z}_{DR} ,
- δ intrinsic differential backscatter phase,
- A_H, A_D intrinsic absolute and differential attenuation,
- \hat{A}_H, \hat{A}_D estimates of A_H and A_D based on $\hat{\Phi}_{DP}$.

The proposed correction procedure is illustrated in Fig. 6: we use Φ_{DP}^M as the first estimate of Φ_{DP} at all range gates. Subsequently, this value is used to estimate A_H and A_D using Eqs. (13)–(17). The values of Z_H^M and Z_{DR}^M at all the range gates are then corrected by estimates $\hat{A}_H(r)$ and $\hat{A}_D(r)$ as follows:

$$\hat{Z}_H(r) = Z_H^M(r) + \hat{A}_H(r), \quad (19)$$

$$\hat{Z}_{DR}(r) = Z_{DR}^M(r) + \hat{A}_D(r). \quad (20)$$

The attenuation-corrected estimate \hat{Z}_{DR} is used to estimate $\hat{\delta}$ using (15). The measured Φ_{DP}^M is then corrected by the estimate $\hat{\delta}$ as

$$\hat{\Phi}_{DP} = \Phi_{DP}^M - \hat{\delta}. \quad (21)$$

Subsequently, the specific differential phase due to the propagation is estimated from $\hat{\Phi}_{DP}$ as

$$\hat{K}_{DP} = \frac{\Delta \hat{\Phi}_{DP}}{\Delta r}. \quad (22)$$

This procedure can be applied iteratively to attain convergence. As shown in Fig. 6 the iteration terminates as soon as the difference between two consecutive estimates of Φ_{DP} becomes lower than a fixed threshold TH. In the next section, however, simulations illustrate that even one-step application of this procedure can improve the estimates R_{DR} and R_{DP} significantly. We need to note here that Φ_{DP}^M is used as the first estimate of Φ_{DP} , neglecting δ . This is likely to create poorer estimates in the front end of the storm. This arises from the fact that (Φ_{DP}, A_H, A_D) are effectively range-integrated values of $(K_{DP}, \alpha_H, \alpha_D)$, respectively. Consequently, the scatters between the $(A_H, A_D) - \Phi_{DP}$ relationships behave similarly to those between $(\alpha_H, \alpha_D) - K_{DP}$ relationships over short paths. But over longer paths the standard errors of A_H and A_D are smaller than those for smaller paths. Thus, it is better to initiate the correction procedure after a few degrees of Φ_{DP} accumulation in range. This procedure with the lack of correction over the first few range gates is not detrimental.

5. Evaluation of the correction procedure

The effectiveness of the correction procedure in improving the rain-rate estimates at a given measurement cell depends on the rainfall path between the radar and the measurement cell. If the attenuation is not significant, then the correction process may introduce more error than using the slightly attenuated Z_H and Z_{DR} in the rainfall estimates (Aydin et al. 1989). Note also that if the parameter δ along the range profile is fairly constant, then the estimates of K_{DP} are not affected, even if the absolute and differential attenuations are significant. Furthermore, different types of range profiles can produce similar net accumulated attenuations and phase shifts. In order to deal with these various possibilities, we study a standard 1-km path with varied

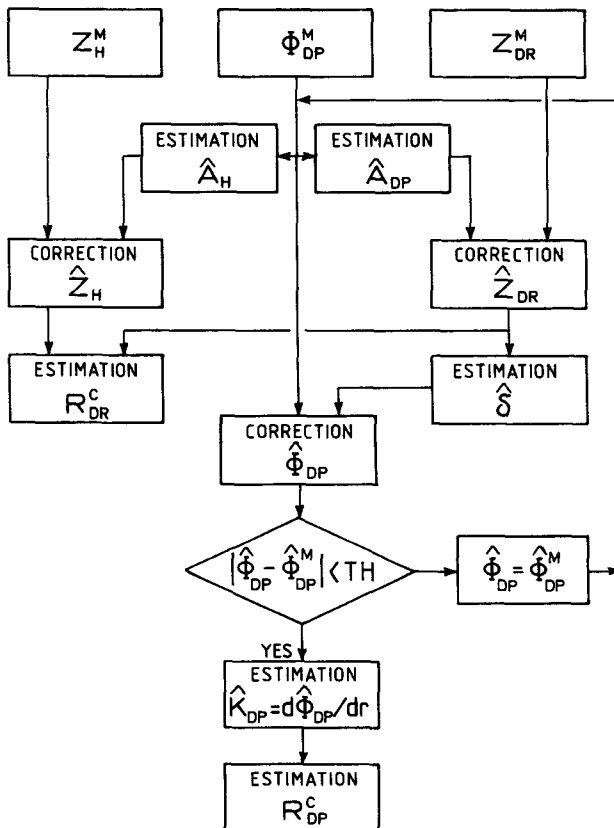


FIG. 6. Schematic of the correction procedure.

reflectivity levels and polarimetric parameters such as Z_{DR} and K_{DP} . By observing the correction procedure over this standardized situation, the performance can be analyzed and extended to evaluate the accuracy over any given range profile.

In the following analysis we examine two different rainfall paths that give different values of attenuation from very small to large values, existing in paths where the RSD remain constant in one case and vary in the second case. In each situation the accuracy of corrected rainfall rates is shown to depend on the extent of attenuation and the effectiveness of the associated correction procedure.

a. Uniform rainfall path

Uniform rainfall paths occur occasionally in many practical meteorological situations. They can also provide important insight into the procedures considered here. One of the ways to achieve approximately uniform rainfall path is by considering short ranges. In the case of uniform rain medium Z_H , Z_{DR} , K_{DP} , and δ are constant with the range. When δ is constant along the range, the estimate of K_{DP} from a profile of Φ_{DP} or $\Phi_{DP} + \delta$ will be the same. Thus, correcting for δ may be worse than using an uncorrected Φ_{DP} ; K_{DP} can be estimated using a simple finite-difference scheme as

$$\hat{K}_{DP} = \frac{\Phi_{DP}^M(r_{i+1}) - \Phi_{DP}^M(r_i)}{2(r_{i+1} - r_i)}, \quad (23)$$

where $\Phi_{DP}^M(r_{i+1})$ and $\Phi_{DP}^M(r_i)$ represent the measured Φ_{DP} at range r_{i+1} and r_i , respectively. Note that the estimate of K_{DP} can be improved by using the linear regression line (Zrnić et al. 1989) or polynomial fit (Golestani et al. 1989) through the profile of Φ_{DP} . We can see from (23) that \hat{K}_{DP} is the same even if $\delta \neq 0$, since a constant δ would cancel in the expression. Similarly, K_{DP} can be estimated using (23) but replacing Φ_{DP}^M by $\hat{\Phi}_{DP}$.

The correction procedure is analyzed from simulations of uniform rainfall rate over paths 1 km long and composed of different RSD. These paths are uniform with the same RSD throughout and we observe Z_H and Z_{DR} sampled at the end of the 1-km path which has experienced attenuation, and differential attenuation, respectively. The Φ_{DP} measurement is perturbed by the value of δ at the same range where Z_H and Z_{DR} are sampled. We define the following variables for this purpose:

- R_{DR}^U estimate of rain rate using Z_H^M and Z_{DR}^M uncorrected,
- R_{DP}^U estimate of rain rate using K_{DP}^M obtained without correcting Φ_{DP}^M for δ ,
- R_{DR}^C estimate of rain rate using \hat{Z}_H and \hat{Z}_{DR} after correction for attenuation,
- R_{DP}^C estimate of rain rate using \hat{K}_{DP}^M obtained from $\hat{\Phi}_{DP}$ after correcting for δ .

Generally R_{DR}^U underestimates the true rainfall R because the decrease of Z_H due to the absolute attenuation is higher than the corresponding decrease of Z_{DR} due to differential attenuation. However, for rain rates greater than 200 mm h⁻¹, R_{DR}^U overestimates R because the measured Z_{DR} becomes very small due to the differential attenuation. On the other hand at low rain rates, R_{DR}^C overestimates R because of the scatter around the mean relationship between the absolute and differential attenuation versus differential phase constant (see Figs. 4a and 4b). We can analyze the accuracy of the correction technique by evaluating the standard errors $\epsilon(R_{DR}^U)$ and $\epsilon(R_{DR}^C)$, corresponding to the estimates R_{DR}^U and R_{DR}^C normalized to the mean value of R . This is illustrated in Fig. 7 for intervals of R equal to 20 mm h⁻¹. We can note slight improvements in the estimates of R mainly for the range of rain rates between 90 and 150 mm h⁻¹; for rain rates between 0 and 90 mm h⁻¹ the correction process introduces greater error than using the attenuated (Z_H , Z_{DR}). Moreover, $\epsilon(R_{DR}^U)$ does not significantly depend on rainfall rate, while $\epsilon(R_{DR}^C)$ decreases with increasing rain in the similar way as the normalized standard error of the intrinsic estimate R_{DR} shown in Fig. 2.

Figure 8 shows the standard errors $\epsilon(R_{DP}^U)$ and $\epsilon(R_{DP}^C)$ as a function of rainfall rate. Comparing the plots in Figs. 8 and 2 we can see that the estimate R_{DP}^U performs as well as expected theoretically since for uniform rainfall paths estimates of K_{DP} are not affected by δ . However, the effect of the correction procedure for Φ_{DP} in uniform rainfall path can be observed

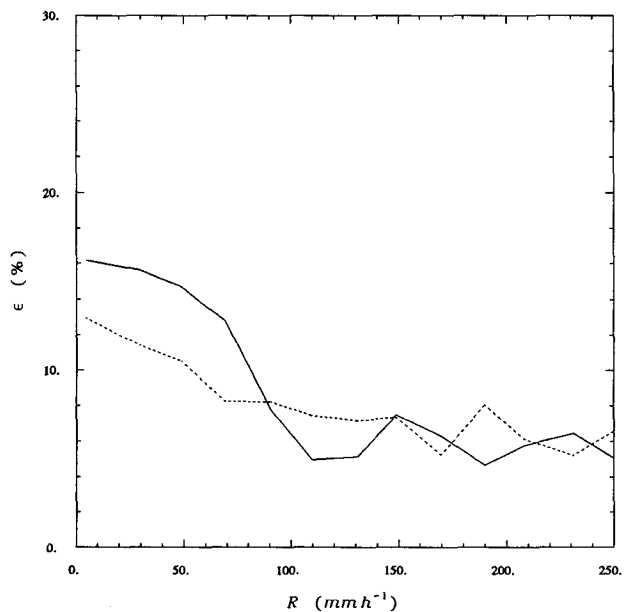


FIG. 7. Normalized standard error ϵ (%) as a function of the actual rain rate R in the uniform rain case. The dotted line refers to the standard error of the uncorrected estimate R_{DR}^U and the solid line to the standard error of the corrected estimate R_{DR}^C .

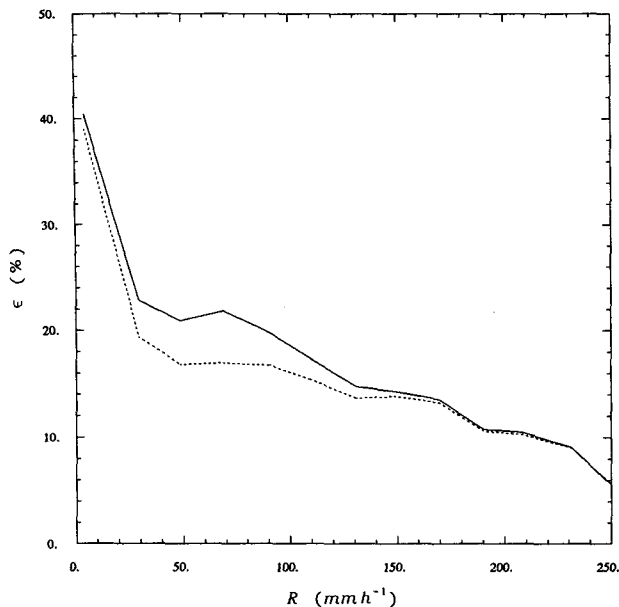


FIG. 8. Normalized standard error ϵ (%) as a function of the actual rain rate R in the uniform rain case. The dotted line refers to the standard error of the uncorrected estimate R_{DP}^U and the solid line to the standard error of the corrected estimate R_{DP}^C .

from Fig. 8 where $\epsilon(R_{DP}^C)$ are slightly higher than the values corresponding to uncorrected estimates. The comparison of the plots in Figs. 7 and 8 shows that, except at the highest rates, the estimate R_{DR}^C is more accurate than the corresponding estimate R_{DP}^C , in agreement with the results obtained for the intrinsic estimates in Fig. 2. The estimates R_{DR}^C and R_{DP}^C perform equally well at high rain rates. However, note that increasing the length of uniform rain path reduces the accuracy of R_{DR} estimates due to the effects of cumulative attenuations.

In order to simulate the effects of measurement errors on the radar observables Z_H , Z_{DR} , and K_{DP} we utilize the procedure of Chandrasekar et al. (1986). The principal parameters of the estimates are as follows: (a) wavelength, $\lambda = 5.5$ cm; (b) sampling time, $T_s = 1$ ms; (c) number of sample pairs, $N = 128$; (d) Doppler velocity spectrum with Gaussian width $w = 2$ m s⁻¹; (e) zero lag cross correlation between H and V signals, $\rho_{HV}(0) = 0.99$.

The estimates of Z_H and Z_{DR} are obtained as

$$Z_H = \frac{1}{N} \sum_{i=1}^N (P_H)_{2i}, \quad (24)$$

$$Z_{DR} = \frac{\sum_{i=1}^N (P_H)_{2i}}{\sum_{i=1}^N (P_V)_{2i+1}}, \quad (25)$$

where P_H, P_V are samples proportional to backscattered

power. The differential phase shift is estimated using the dual polarized pulse pair algorithm (Mueller 1984; Sachidananda and Zrnić 1986)

$$\hat{\Phi}_{DP} = \frac{1}{2} (\psi_1 - \psi_2), \quad (26)$$

where

$$\psi_1 = \arg \sum H_{2i} V_{2i+1}^*, \quad (27)$$

and

$$\psi_2 = \arg \sum V_{2i+1}^* H_{2i+2}, \quad (28)$$

where H_{2i} and V_{2i+1} are the coherent complex time samples at time instants $2i$ and $2i + 1$.

Figure 9 shows the standard errors $\epsilon(R_{DR}^C)$ and $\epsilon(R_{DP}^C)$ versus R , where the measurement error is superimposed. As expected, the measurement fluctuation increases both $\epsilon(R_{DR}^C)$ and $\epsilon(R_{DP}^C)$. We can see from this plot that R_{DR}^C outperforms R_{DP}^C at values of R up to around 120 mm h⁻¹. For $120 < R < 180$ mm h⁻¹ both R_{DR}^C and R_{DP}^C exhibit comparable errors, and for $R > 180$ mm h⁻¹, R_{DP}^C outperforms R_{DR}^C . We also note that this boundary will move to lower rain rates if we extend the path over which K_{DP} is estimated to be larger than 1 km.

b. Nonuniform rainfall path

The nonuniform rainfall case is simulated by examining both negative and positive linear variation of

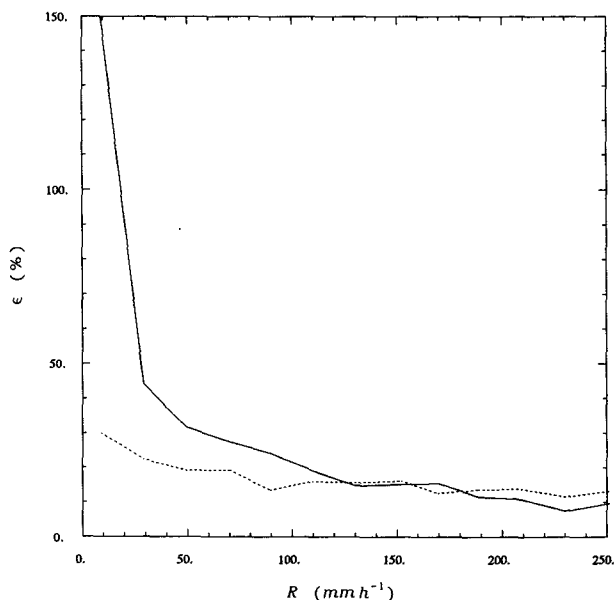


FIG. 9. Normalized standard error ϵ (%) with superimposed measurement error as a function of the actual rain rate R in the uniform rain case. The dotted line refers to the standard error of the corrected estimate R_{DR}^C and the solid line to the standard error of the corrected estimate R_{DP}^C .

the median volume diameter D_0 along the path with range interval $\Delta x = 1$ km for each of the RSD given in section 2. Thus in addition to a random variability of D_0 between 0.5 and 2.5 mm, we have superimposed a linear variability of D_0 described by a triangular probability density function that ranges between -2 and 2 mm km $^{-1}$. The estimate of the differential phase constant is still obtained through (23). Unlike the uniform rain case, the parameter δ is not constant; hence, the perturbation of K_{DP} estimates due to δ can differ from zero. For negative gradients of D_0 , the variation of δ is negative and for low rain rates this decrease in δ can be larger than the positive increase in differential phase shift due to propagation. Measurement errors are not included here to focus on the effects of non-uniform rain paths. Figure 10 shows the normalized standard errors $\epsilon(R_{DP}^U)$ and $\epsilon(R_{DP}^C)$ versus R ; we can see that $\epsilon(R_{DP}^U)$ increases greatly in the range of 0–200 mm h $^{-1}$ where R_{DP}^U significantly overestimates R . For high rain rates the perturbation of δ is less important to the estimate of K_{DP} so that the uncorrected measurement approximates very closely the intrinsic value of K_{DP} . The results shown in Fig. 10 indicate that the correction procedure performs fairly well over the full range of rain rates, and the normalized standard errors of R_{DP}^C approximate closely those corresponding to the uniform rain case. The difference between $\epsilon(R_{DP}^U)$ and $\epsilon(R_{DP}^C)$ is a useful parameter for determining whether applying the correction procedure is better than leaving the data uncorrected for attenuation. This difference varies from +2% to 30% indicating that correcting for δ is useful in improving estimates of R .

6. Conclusions

We have developed expressions for C-band rainfall estimates using the dual polarization reflectivity-based technique (R_{DR}) and the dual polarization phase-based technique (R_{DP}) by varying parameters of the raindrop size distributions (RSD) over a wide range of natural rainfall. The effects of measurement errors due to signal fluctuations on the normalized standard error of R_{DR} and R_{DP} are presented. For rain rates in excess of 100 mm h $^{-1}$, the average standard errors of R_{DR} and R_{DP} are comparable, whereas at rain rates less than 100 mm h $^{-1}$, R_{DR} outperforms R_{DP} . The effects of propagation and differential backscatter phase shift δ on the various estimates at C-band frequencies are shown to be significant with absolute and differential attenuations through typical rainfall situations being of the order of several decibels and a couple of decibels, respectively, and δ can be as large as 15°.

An iterative procedure to correct the radar observables (Z_H , Z_{DR}) for (A_H , A_D) and Φ_{DP} for δ is described; it is based on the mean relationships between the differential phase constant K_{DP} and the absolute and differential attenuation as well as Z_{DR} and δ . We have evaluated the effectiveness of the technique for two

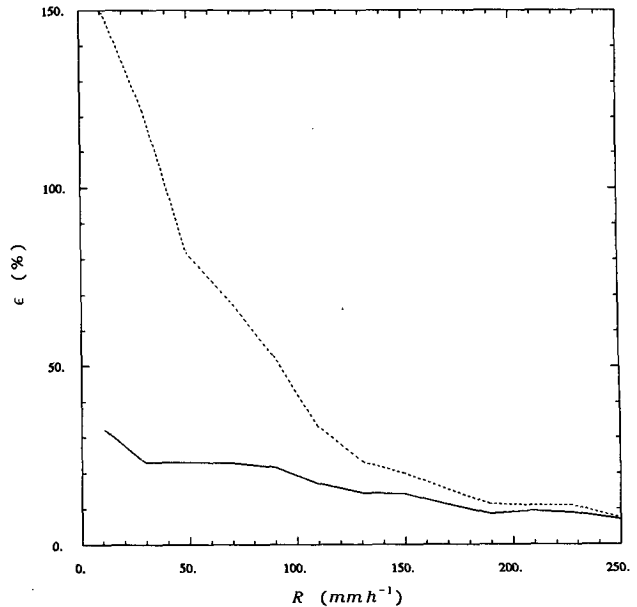


FIG. 10. Normalized standard error ϵ (%) as a function of the actual rain rate R in the case of nonuniform rainfall path. The dotted line refers to the standard error of the uncorrected estimate R_{DP}^U and the solid line to the standard error of the corrected estimate R_{DP}^C .

different types of rain medium, one where the rain path remains uniform and the other where the path is non-uniform. In the case of uniform rain path the mean value of the radar observables and the parameter δ are constant. When δ is constant with range, K_{DP} estimated from a profile of Φ_{DP} or $\Phi_{DP} + \delta$ will be the same, suggesting that attempting to correct for δ may produce greater error than using an uncorrected Φ_{DP} . We have shown that the normalized standard error of the corrected estimate of R_{DP} is nearly the same as the uncorrected estimate. The corrected estimates of R_{DR} show some improvement in the range of rain rates between 80 and 150 mm h $^{-1}$. For rain rates between 0 and 80 mm h $^{-1}$, the correction process appears to introduce more error than using the attenuation-affected (Z_H , Z_{DR}). Based on 1-km path estimates of K_{DP} , the estimates of R_{DR} are found to be more accurate than R_{DP} over the range of rain rates between 0 and 150 mm h $^{-1}$.

Nonuniform rainfall paths are obtained by simulating increases and decreases of the median volume diameter D_0 so that the estimation of K_{DP} is perturbed by δ . We have shown that the correction procedure performs well in the full range of rainfall variability considered here, yielding an improvement ranging from 2% to 30%, depending on the variation of δ along the path. The estimates of R_{DR} demonstrate accuracies quite similar to those obtained in the uniform rain case after correction for propagation effects. Our simulations have been performed for an ideal situation, namely, with the radar sampling a homogeneous resolution

volume. Under such conditions we have evaluated the problems associated with rainfall estimation using C-band radars. We recognize that several physical factors such as a nonuniform resolution cell, partial beam filling, and advection of rain cell will affect all the estimates of rainfall based on radar measurements. Nevertheless the results of this simulation reinforce the efficacy of utilizing C-band radar for rainfall estimation by examining the specific behavior of dual polarization radar parameters and showing that, similar to previous studies by Hildebrand (1978) and Aydin et al. (1989), compensation for attenuation is feasible. The results have been extended to differential phase measurements, demonstrating that corrections for variations by δ are possible for improving rainfall estimates from K_{DP} .

Acknowledgments. This research was supported by the National Group for Defense from Hydrogeological Hazards (CNR-Italy) and the USARO through the Center for Geosciences at Colorado State University and by The Pennsylvania State University (subcontract to University of Washington). We thank one of the reviewers whose comments greatly improved the paper, especially the Appendix.

APPENDIX

Simplified Correction Procedure for Z_H , Z_{DR} , and ϕ_{DP}

We have seen in the main text that measurements of Z_H and Z_{DR} are perturbed by attenuation and differential attenuation whereas measurements of ϕ_{DP} are perturbed by δ . The attenuation and differential attenuation can be potentially corrected from estimates of ϕ_{DP} that are unaffected by δ . Repeating Eqs. (19)–(21) from the main text we have

$$\hat{Z}_H(r) = Z_H^M(r) + \hat{A}_H(r), \tag{A1}$$

$$\hat{Z}_{DR}(r) = Z_{DR}^M(r) + \hat{A}_D(r), \tag{A2}$$

$$\hat{\Phi}_{DP} = \Phi_{DP}^M - \hat{\delta}. \tag{A3}$$

We can also write an estimate of $A_D(r)$ using (14) of main text as

$$A_D(r) = C_D \phi_{DP}, \tag{A4}$$

where $C_D = 0.013$ at C band. The relationship between δ and Z_{DR} seen in Fig. 5 can be simplified into a second-degree polynomial of the form

$$\delta = a_0 + a_1 Z_{DR} + a_2 Z_{DR}^2, \tag{A5}$$

where a_0 , a_1 , and a_2 are the coefficients of the polynomial regression. At C-band frequencies a_0 , a_1 , and a_2 take the values 0.9302, -2.2492 , and 1.1633, respectively. Substituting (A4) and (A2) into (A5) we get

$$\delta = a_0 + a_1(Z_{DR}^M + C_D \phi_{DP}) + a_2(Z_{DR}^M + C_D \phi_{DP})^2; \tag{A6}$$

(A6) when substituted into (A3) gives

$$\phi_{DP} = \phi_{DP}^M - a_0 - a_1(Z_{DR}^M + C_D \phi_{DP}) - a_2(Z_{DR}^M + C_D \phi_{DP})^2, \tag{A7}$$

which can be simplified into

$$\phi_{DP}^2(C_D^2 a_2) + \phi_{DP}(1 + 2a_2 C_D + a_1 C_D) + [a_0 + a_1 Z_{DR}^M + a_2(Z_{DR}^M)^2 - \phi_{DP}^M] = 0. \tag{A8}$$

We can see that the above equation is a quadratic in ϕ_{DP} and can be solved explicitly. We can write (A8) as

$$A \phi_{DP}^2 + B \phi_{DP} + C = 0, \tag{A9}$$

where

$$A = C_D^2 a_2,$$

$$B = 1 + 2a_2 C_D + a_1 C_D,$$

$$C = a_0 + a_1 Z_{DR}^M + a_2(Z_{DR}^M)^2 - \phi_{DP}^M.$$

Under this notation the solution for ϕ_{DP} is

$$\phi_{DP} = \frac{-B \pm (B^2 - 4AC)^{1/2}}{2A}; \tag{A10}$$

ϕ_{DP} obtained through (A10) can be used with (A1) and (A2) to obtain intrinsic values of Z_H and Z_{DR} . We note here that this simplified solution is possible, with a second-degree approximation to the relationship between Z_{DR} and δ .

REFERENCES

Atlas, D., and C. W. Ulbrich, 1977: Path- and area-integrated rainfall measurement by microwave attenuation in the 1–3 cm band. *J. Appl. Meteor.*, **16**, 1322–1331.

Aydin, K., H. Direskeneli, and T. A. Seliga, 1987: Dual-polarization radar estimation of rainfall parameters compared with ground-based disdrometer measurements: October 29, 1982 Central Illinois Experiment. *IEEE Trans. Geosci. Remote Sens.*, **6**, 834–844.

—, Y. Zhao, and T. A. Seliga, 1989: Rain-induced attenuation effects on C-band dual-polarization meteorological radars. *IEEE Trans. Geosci. Remote Sens.*, **24**, 57–63.

Beard, K. V., and C. Chuang, 1987: A new model for the equilibrium shape of raindrops. *J. Atmos. Sci.*, **44**, 1509–1524.

Bringi, V. N., T. A. Seliga, and S. M. Cherry, 1982: First comparisons of rainfall rates derived from radar differential reflectivity and disdrometer measurements. *IEEE Trans. Geosci. Remote Sens.*, **2**, 201–204.

—, V. Chandrasekar, N. Balakrishnan, and D. S. Zrnić, 1990: An examination of propagation effects in rainfall on radar measurements at microwave frequencies. *J. Atmos. Oceanic Technol.*, **8**, 829–840.

Chandrasekar, V., V. N. Bringi, and P. J. Brockwell, 1986: Statistical properties of dual polarized radar signals. Preprints, *23th Conf. on Radar Meteorology*, Snowmass, Amer. Meteor. Soc., 154–157.

—, W. A. Cooper, and V. N. Bringi, 1988: Axis ratios and oscillation of raindrops. *J. Atmos. Sci.*, **45**, 1325–1333.

- , V. N. Bringi, N. Balakrishnan, and D. S. Zrnić, 1990: Error structure of multiparameter radar and surface measurements of precipitation. Part III: Propagation differential phase shift. *J. Atmos. Oceanic Technol.*, **7**, 621–629.
- Golestani, Y., V. Chandrasekar, and V. N. Bringi, 1989: Intercomparison of multiparameter radar measurements. *24th Conf. on Radar Meteorology*, Tallahassee, Amer. Meteor. Soc., 309–314.
- Green, A. W., 1975: An approximation for the shapes of large raindrops. *J. Appl. Meteor.*, **14**, 1578–1583.
- Hildebrand, P. H., 1978: Iterative correction for attenuation of 5 cm radar in rain. *J. Appl. Meteor.*, **17**, 508–514.
- Leonardi, R. M., G. Scarchilli, E. Gorgucci, and C. Goretti, 1984: A C-band advanced meteorological radar developed for CNR-Italy. Preprints, *22nd Conf. on Radar Meteorology*, Zurich, Amer. Meteor. Soc., 238–243.
- Mueller, E. A., 1984: Calculation procedure for differential propagation phase shift. *22nd Conf. on Radar Meteorology*, Zurich, Amer. Meteor. Soc., 397–399.
- Pruppacher, H. R., and R. L. Pitter, 1971: A semi-empirical determination of the shape of cloud and raindrops. *J. Atmos. Sci.*, **28**, 86–94.
- Sachidananda, M., and D. S. Zrnić, 1986: Differential propagation phase shift and rainfall rate estimation. *Radio Sci.*, **21**, 235–247.
- Schroth, A. C., M. S. Chandra, and P. F. Meischner, 1988: A C-band coherent polarimetric radar for propagation and cloud physics research. *J. Atmos. Oceanic Technol.*, **5**, 803–822.
- Seliga, T. A., and V. N. Bringi, 1976: Potential use of the radar reflectivity at orthogonal polarizations for measuring precipitation. *J. Appl. Meteor.*, **15**, 69–76.
- , and V. N. Bringi, 1978: Differential reflectivity and differential phase shift: Application in radar meteorology. *Radio Sci.*, **13**, 271–275.
- Ulbrich, C. W., 1983: Natural variations in the analytical form of raindrop size distributions. *J. Climate Appl. Meteor.*, **22**, 1764–1775.
- Zrnić, D. S., N. Balakrishnan, and M. Sachidananda, 1989: Polarimetric measurements determine the amounts of rain and hail in a mixture. Preprints, *24th Conf. on Radar Meteorology*, Tallahassee, Amer. Meteor. Soc., 393–400.